

Signatures of active region heating and connection to the slow solar wind

Vanessa Polito

Harvard-Smithsonian Center for Astrophysics

Thanks: P. Testa, G. Del Zanna, J. Dudik

Shine meeting, 30th July 2018

Outline

Introduction:

- Active region heating: evidence supporting nanoflare models

Connections between ARs and slow solar wind? :

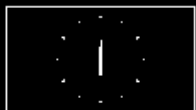
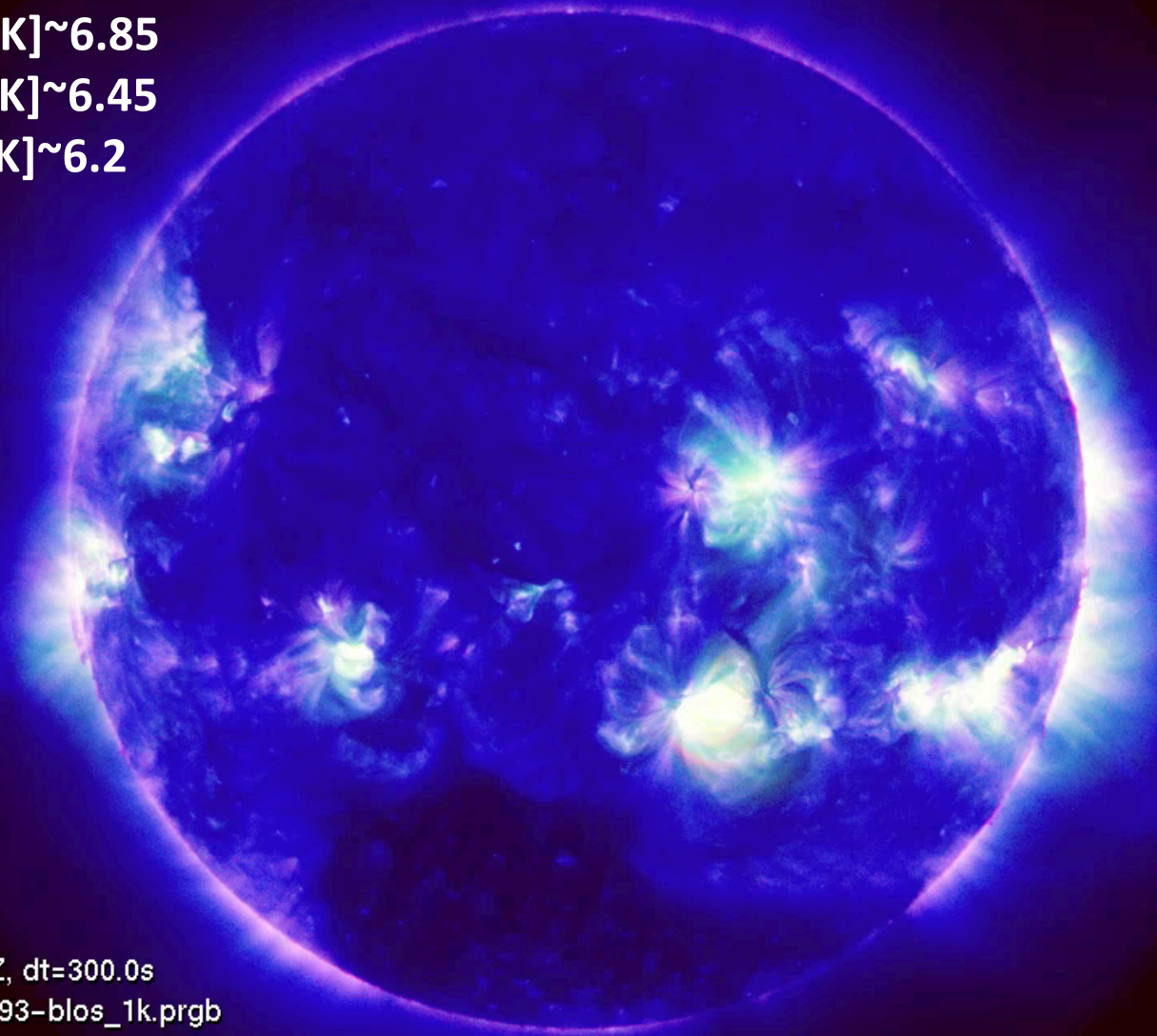
- Flows
- FIP
- magnetic field modeling
- non-Maxwellian distributions

Active region heating

AIA 94, Fe XVIII $\log T[\text{K}] \sim 6.85$

AIA 335, Fe XVI $\log T[\text{K}] \sim 6.45$

AIA 193, Fe XII $\log T[\text{K}] \sim 6.2$



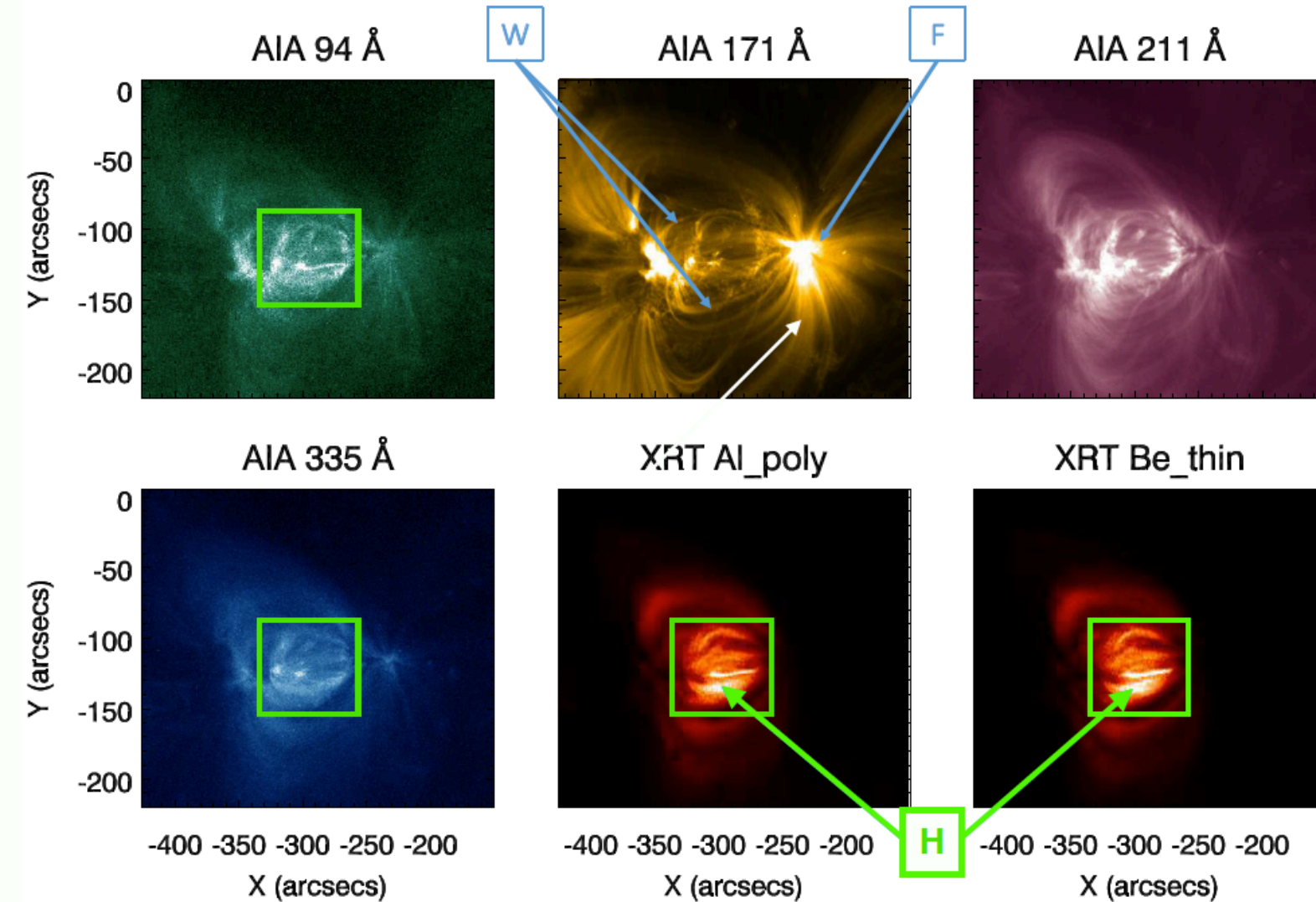
Time: 2014-12-03T18:00:04.826Z, dt=300.0s

aia_20141203T180004_94-335-193-blos_1k.prgb

channel=94, 335, 193, source=AIA,AIA,AIA,HMI

Characteristics of active regions

AR NOAA 12615 in Different Channels



Review by Reale 2015:

- *Cool loops*: detected in UV lines at temperatures between 10^5 and 10^6 K.
- *Warm loops*: observed in most channels of SDO/AIA, confine plasma at $T \sim 1 - 1.5$ MK
- *Hot loops*: typically observed in the X-ray band, and in hot UV and EUV lines (e.g., Fe xvi) and channels (SDO/AIA 335), $T \geq 2$ MK

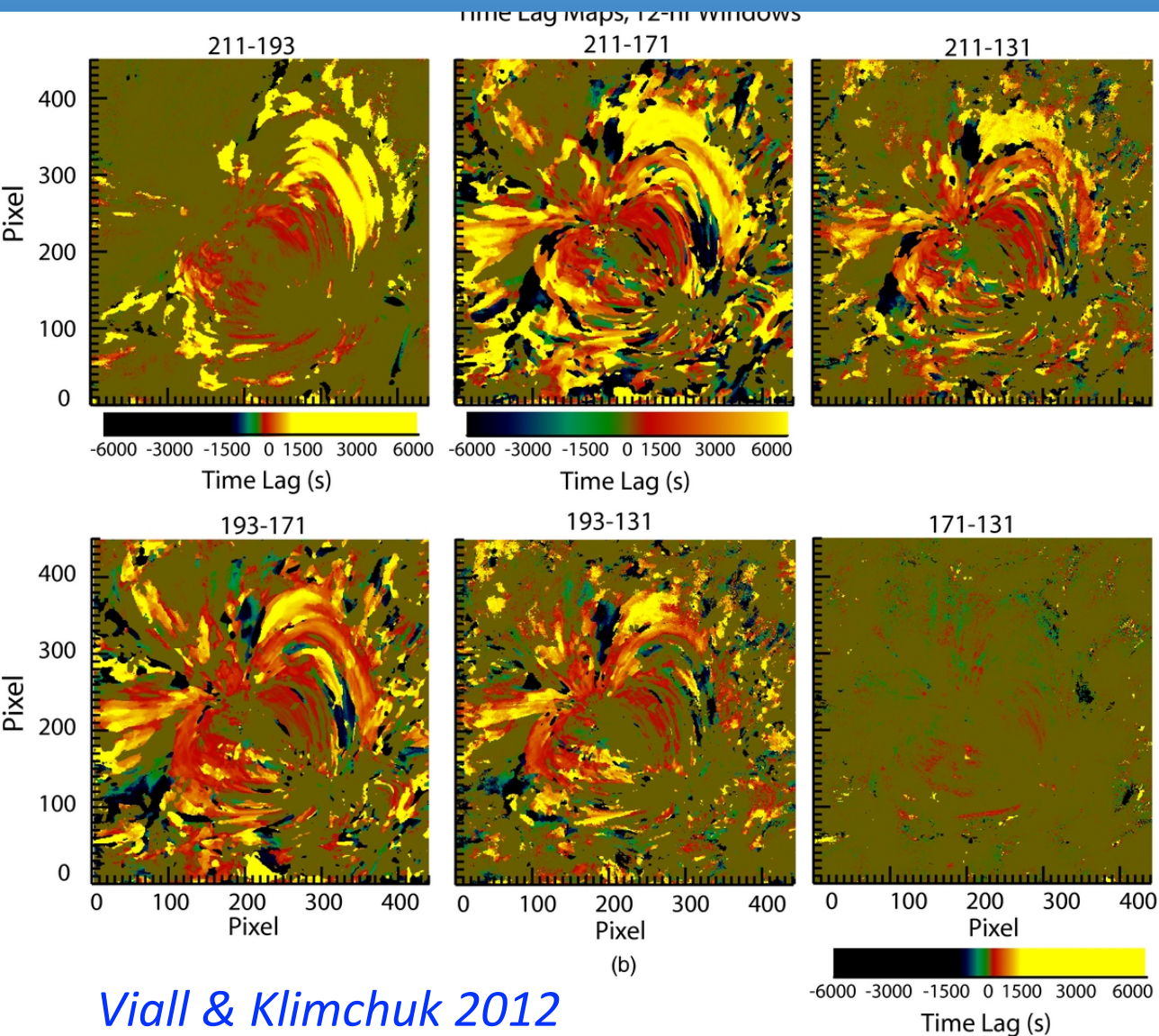
AR heating: open questions

- *How are AR heated?*

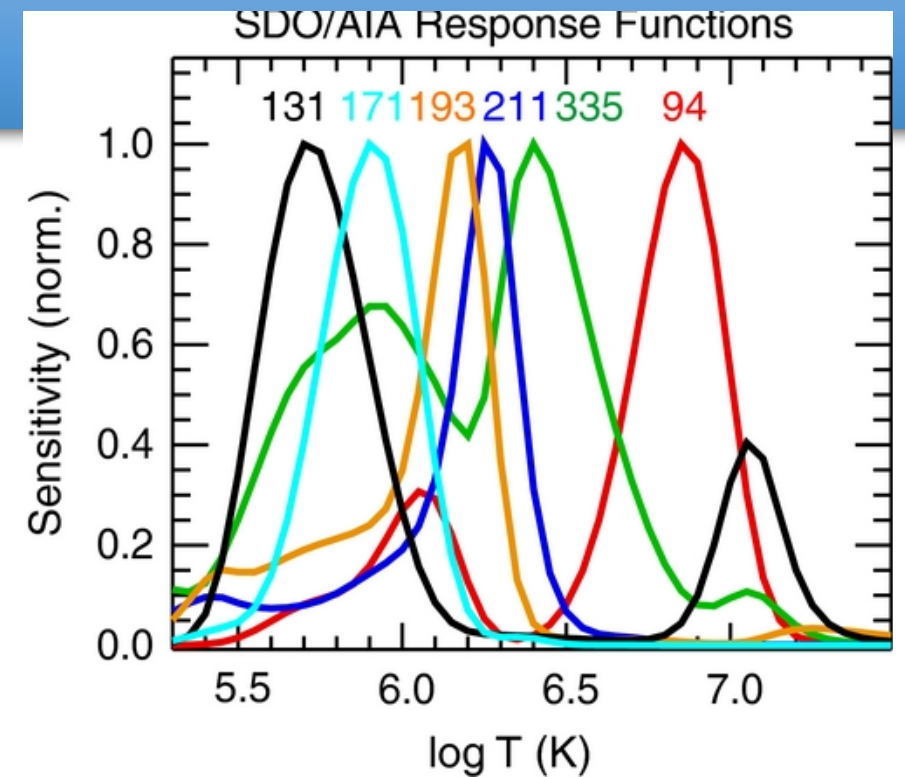
- *Nanoflares*, short bursts of energy release, represent a popular candidate process for converting magnetic energy into the thermal energy required to heat the corona and ARs to millions of degree (see e.g. review by Klimchuk 2006)
- Several recent studies have shown that nanoflare heating is consistent with AR observations (e.g. Viall & Klimchuk, 2012; Testa et al. 2013, 2014, Reep et al. 2013, Brosius et al., 2014; Barnes et al. 2016, Ishikawa et al., 2017).

N.B. The term “nanoflare” may refer to any impulsive release of energy (Klimchuk, 2015), regardless of the underlying driver, whether that be reconnection, Alfvén waves, or some other mechanism

Evidence for nanoflare heating



Viall & Klimchuk 2012



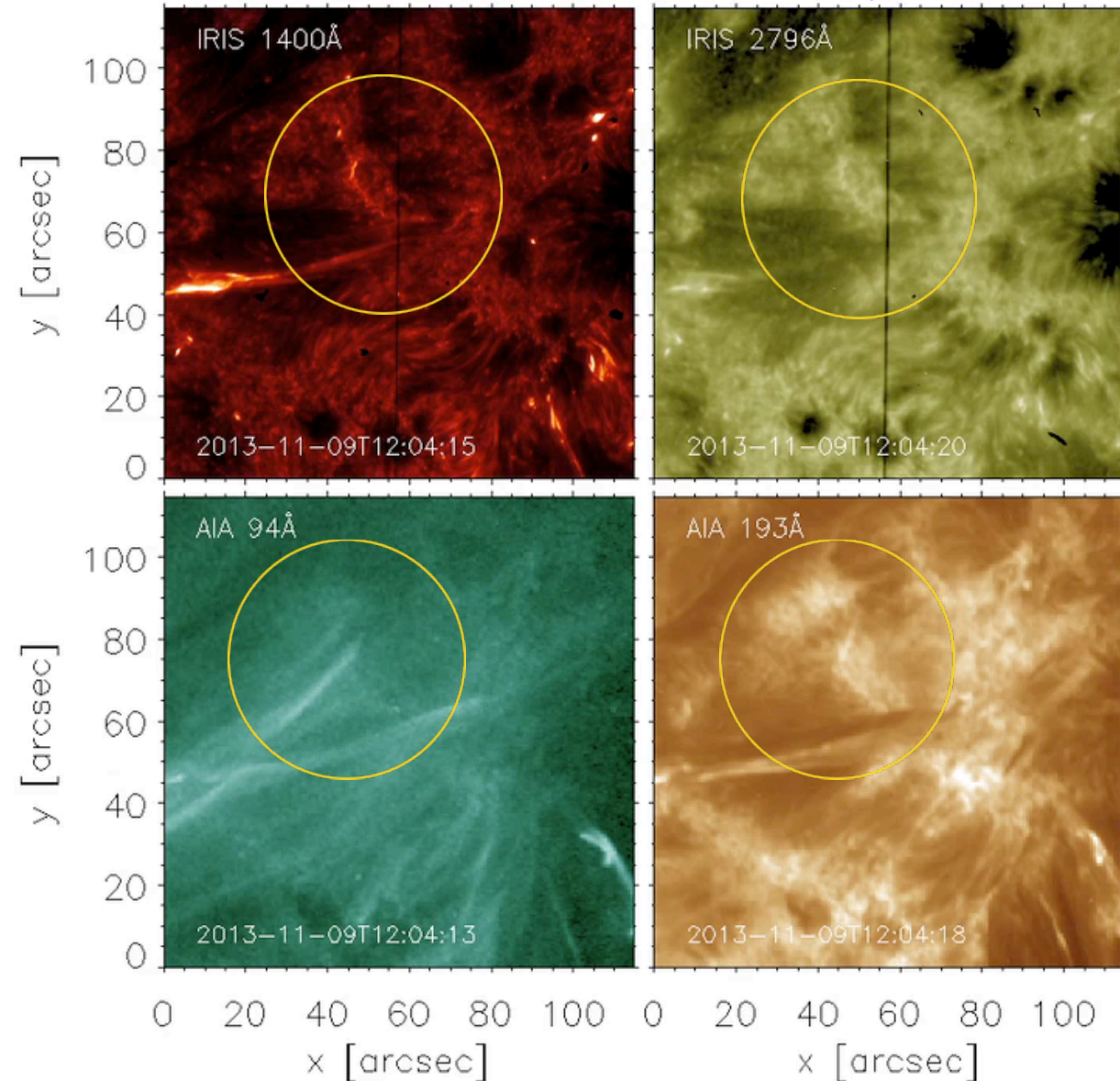
- Time-lag signal consistent with cooling plasma from temperatures of greater than 3 MK, and sometimes exceeding 7 MK, down to temperatures lower than ~ 0.8 MK
- This suggests that the bulk of the emitting coronal plasma in this AR is not steady; rather, it is dynamic and constantly evolving.
- Consistent with nanoflare trains (e.g. Barnes et al. 2016, Reep et al. 2013, Bradshaw et al. 2012)

See Barnes' and Chhabra's posters

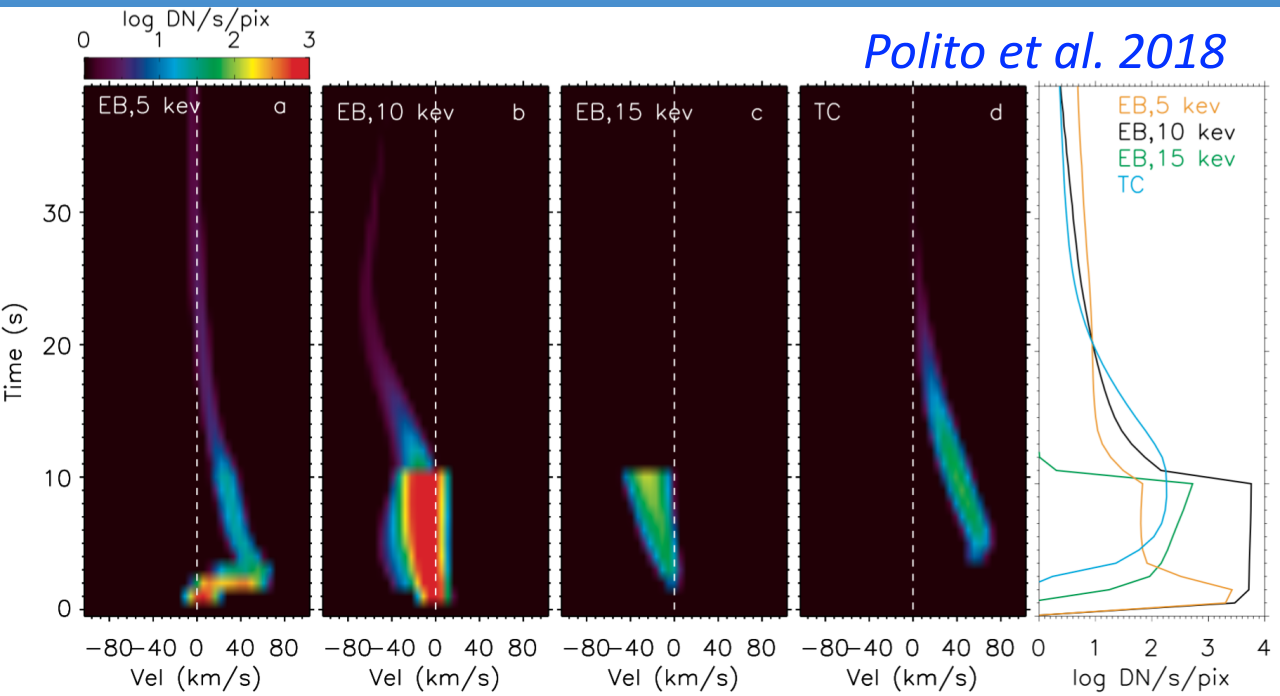
New insights from *IRIS*: constraints on nanoflare models

- Region of rapidly variable mass (~ 10 s) at the footpoints of very hot and dynamic loops as observed by Hi-C and the *Interface Region Imaging Spectrograph* (IRIS)
- These events were interpreted as signatures of heating events associated with reconnection occurring in the overlying hot coronal loops, i.e., coronal nanoflares.
- IRIS Si IV TR spectra ($\log T \sim 4.9$ K) for many brightenings shows modest *blueshift* which could be reproduced assuming heating by *non-thermal electrons (NTE)* with the RADYN code (Carlsson & Stein 97)

Testa et al. 2014, Science



New insights from IRIS: constraints on nanoflare models

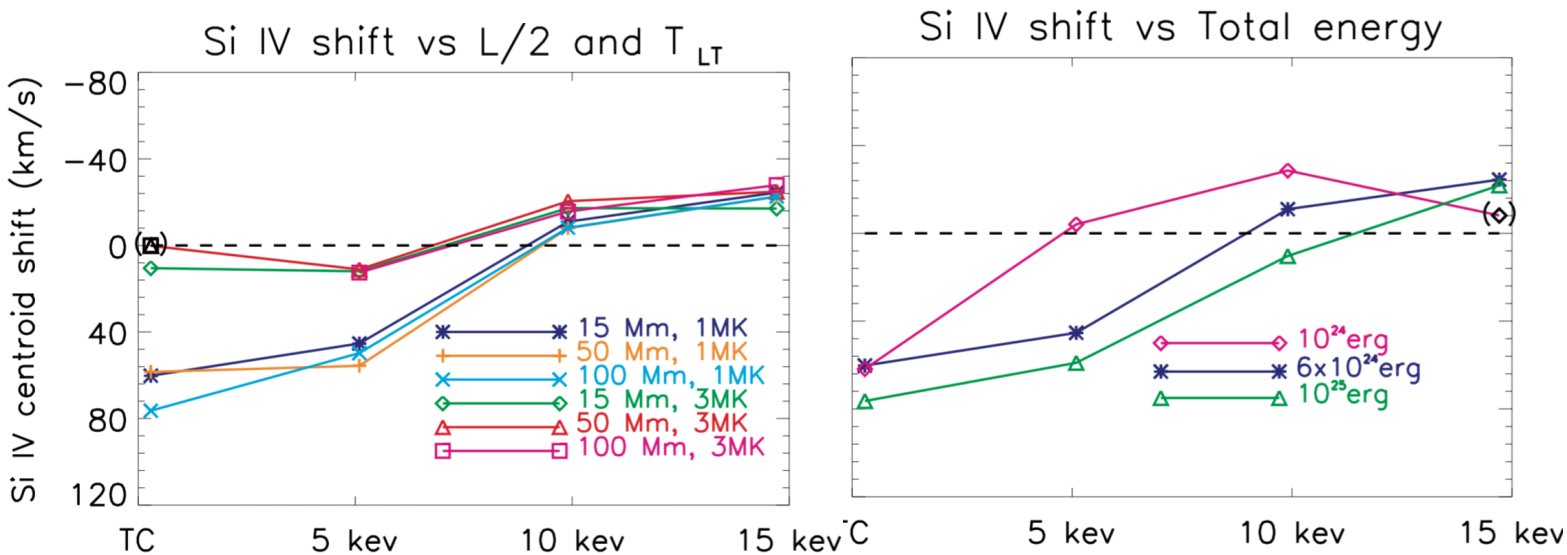


▶ Nanoflare simulations reproduce observed IRIS SiIV intensities and Doppler shift ranges

▶ **Blueshifts** in SiIV only observed for NTE; **redshifts** for thermal conduction (TC) or low-energy NTE— threshold E_c depends on total energy of event

▶ Plasma response depends crucially on initial density

See also Reep, Bradshaw et al. 2013



Outline

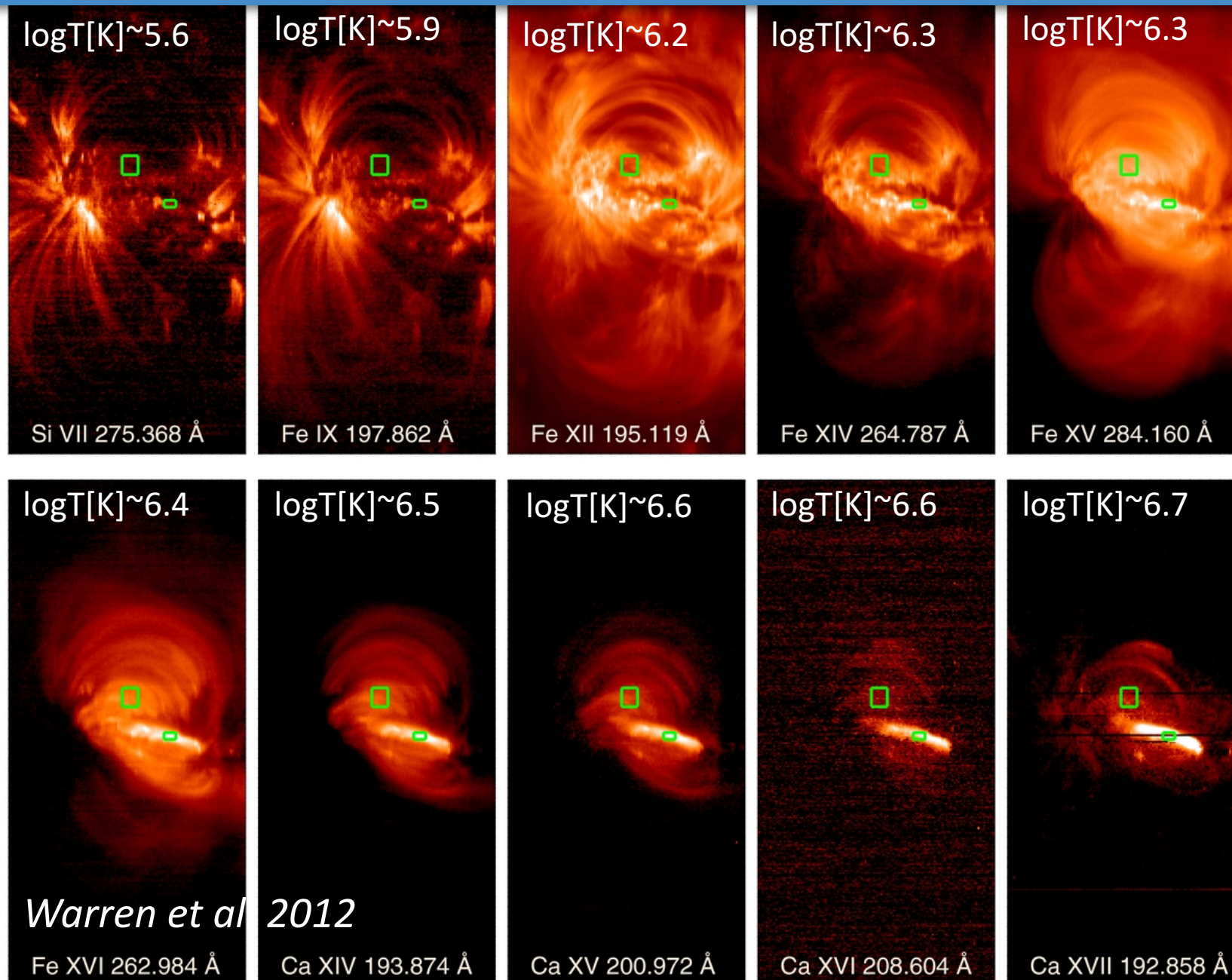
Introduction:

- Active region heating: evidence supporting nanoflare models
(however, the details of the heating mechanisms still highly debated...)

Connections between ARs and slow solar wind? :

- Flows
- FIP
- magnetic field modeling
- non-Maxwellian distributions

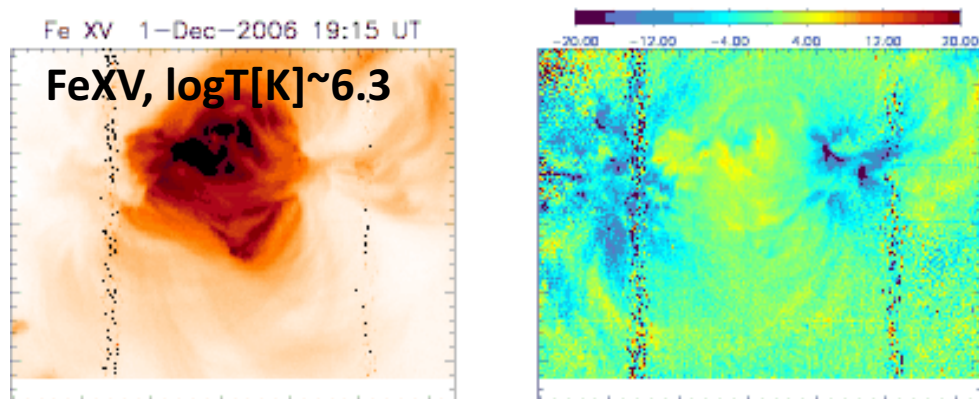
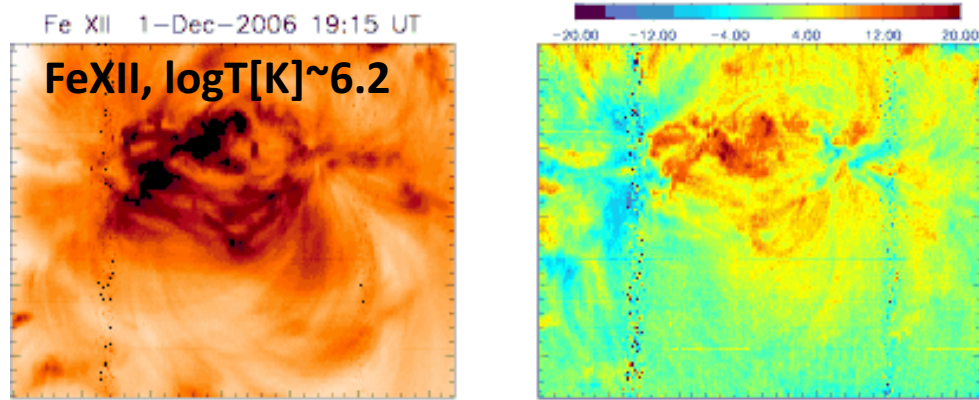
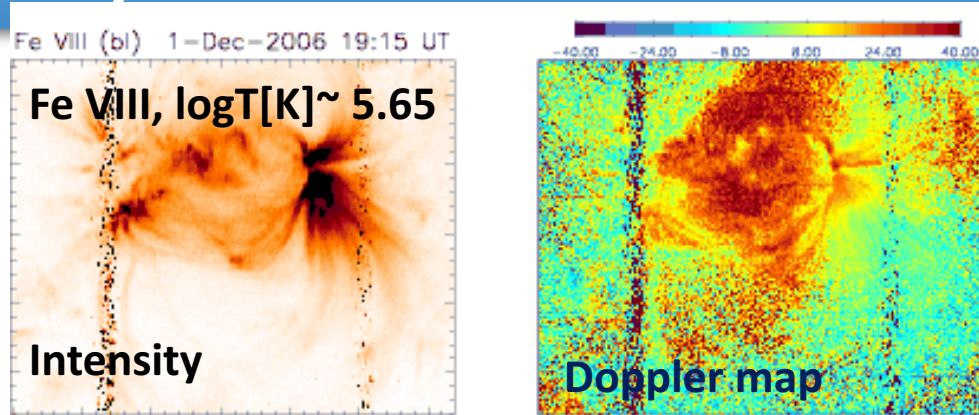
ARs observations with Hinode/EIS



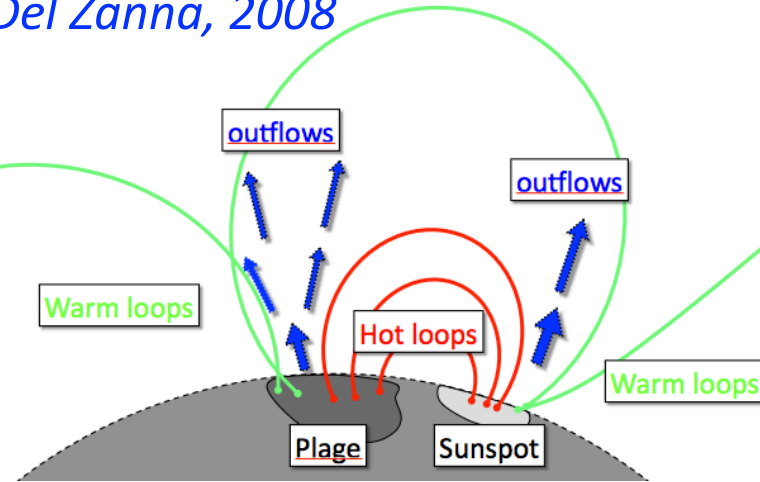
Warren et al 2012

- *Hinode/EIS* has provided many important results on AR heating
- EIS observes ARs over a wide range of temperatures (Fe VIII-Fe XVII) at 2-3'' spatial resolution, providing information about flows, temperatures, density, chemical composition of the emitting plasma

Dynamics in ARs



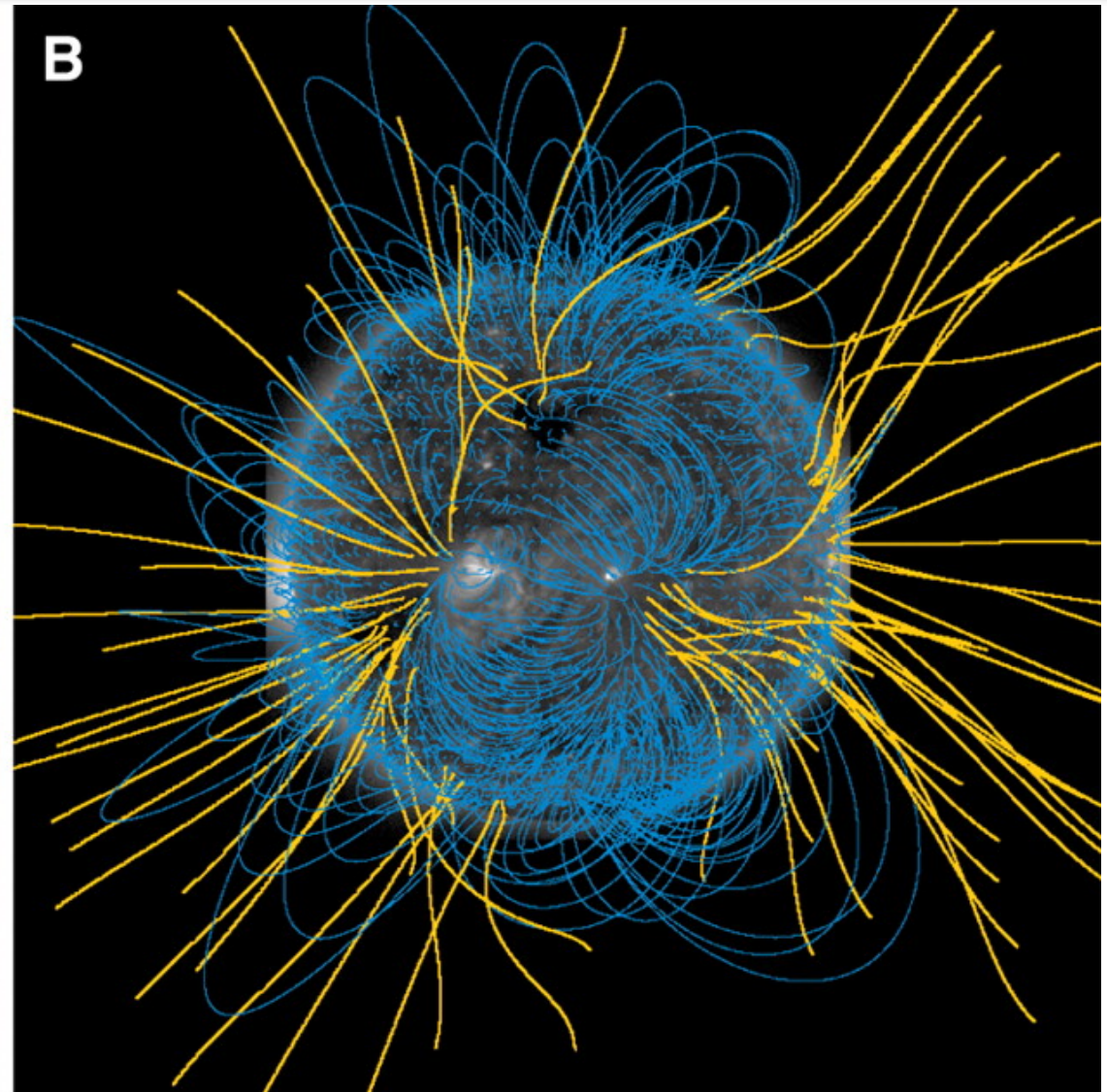
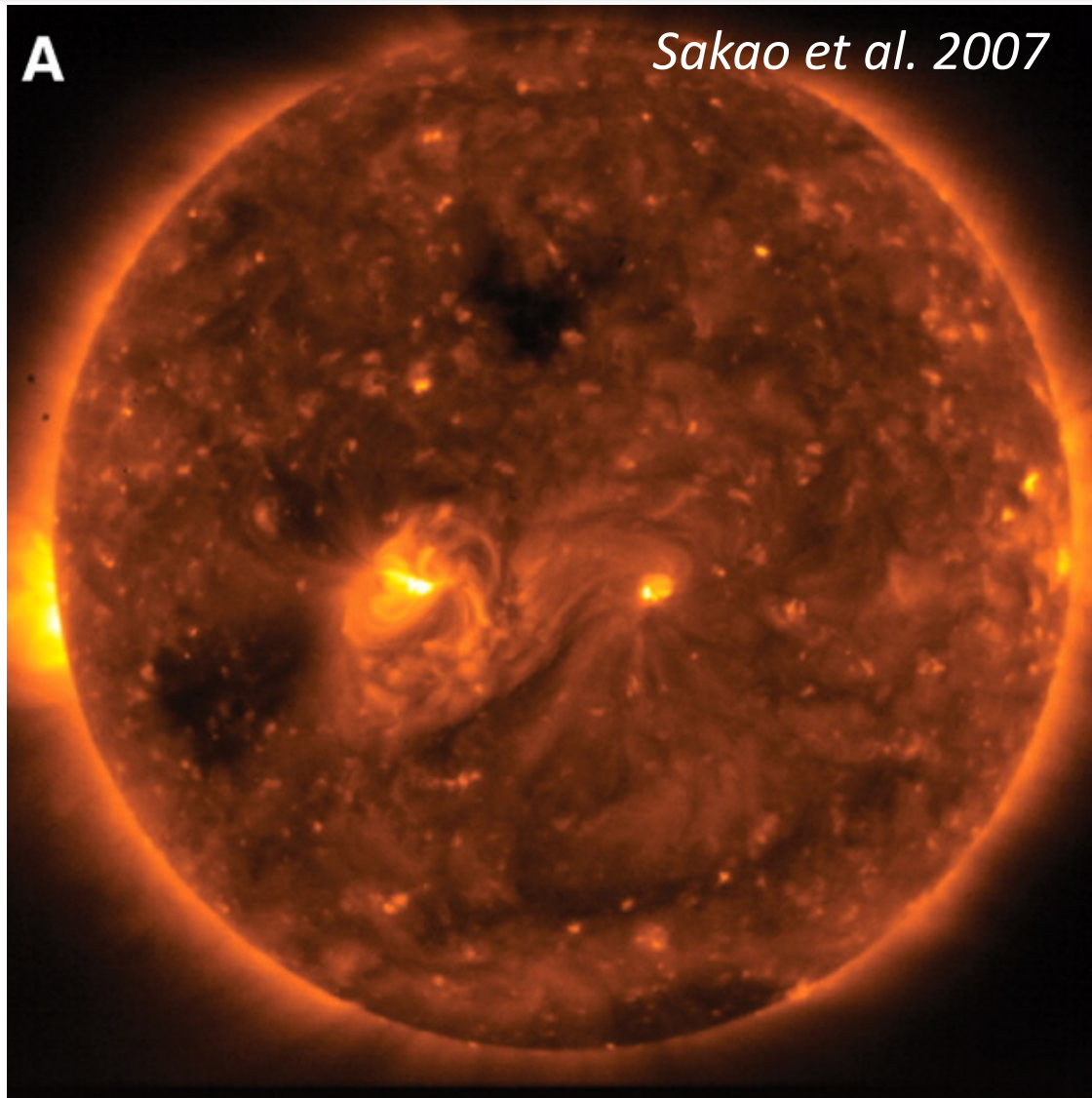
Del Zanna, 2008



High-temperature outflows from the edges of the AR hot core loops (e.g. Sakao 2007, Doschek 2007, Del Zanna 2008, Harra et al. 2008, Doschek et al. 2008, Harra 2017).

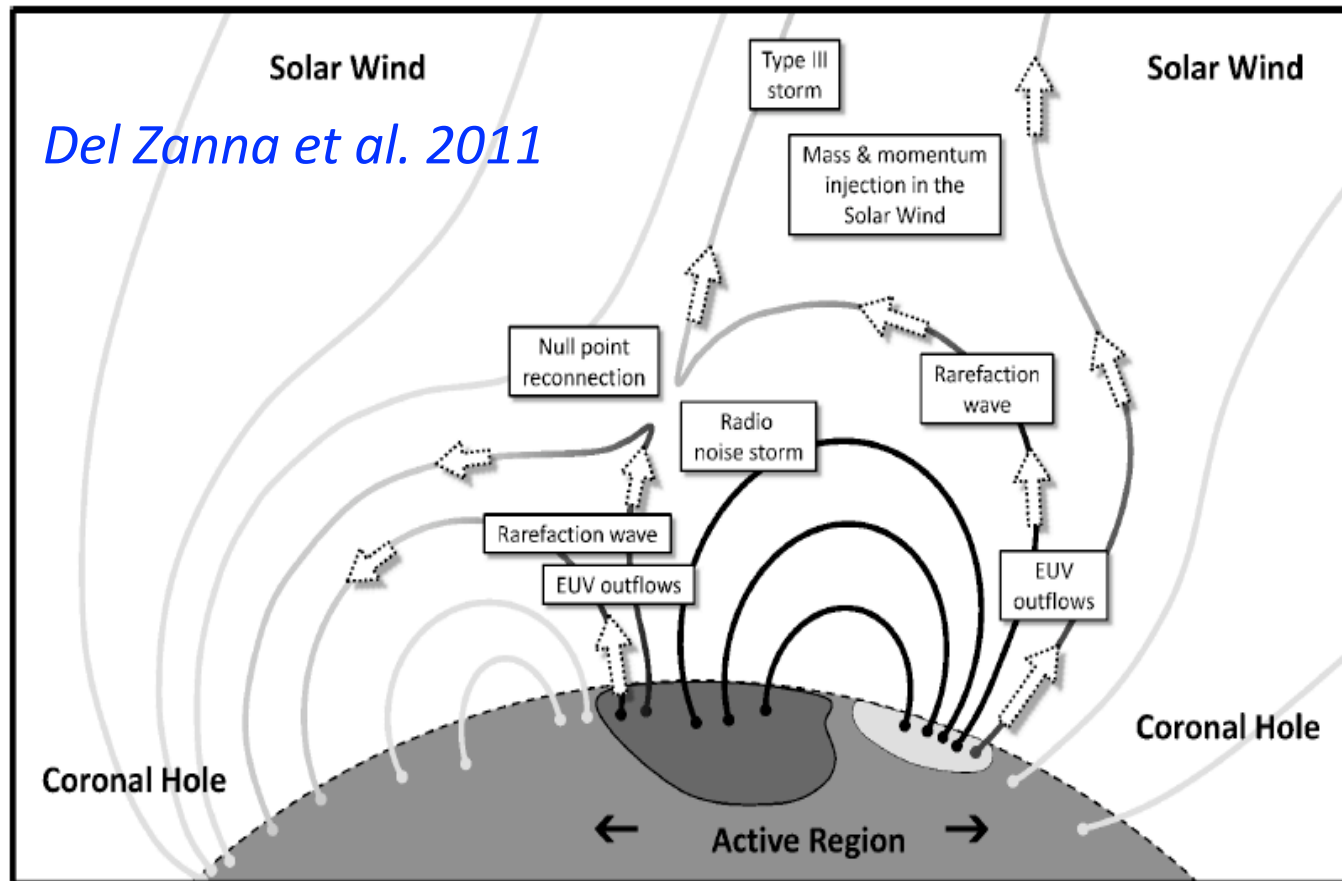
- Shifts are larger in higher-temperature coronal lines. outflows reach velocities of 50 km s^{-1} with line asymmetries reaching 200 km s^{-1} .
- The strongest blueshifts are in low-density regions
- Redshifts prominent in the cooler lines, in almost all loop structures.

AR outflows as possible source of slow solar wind



Outflows may connect to the heliosphere and contribute to the slow wind (Sakao 2007, Harra 2008, Doschek 2008, Baker 2009, Slemzin 2013).

AR outflows as possible source of slow solar wind

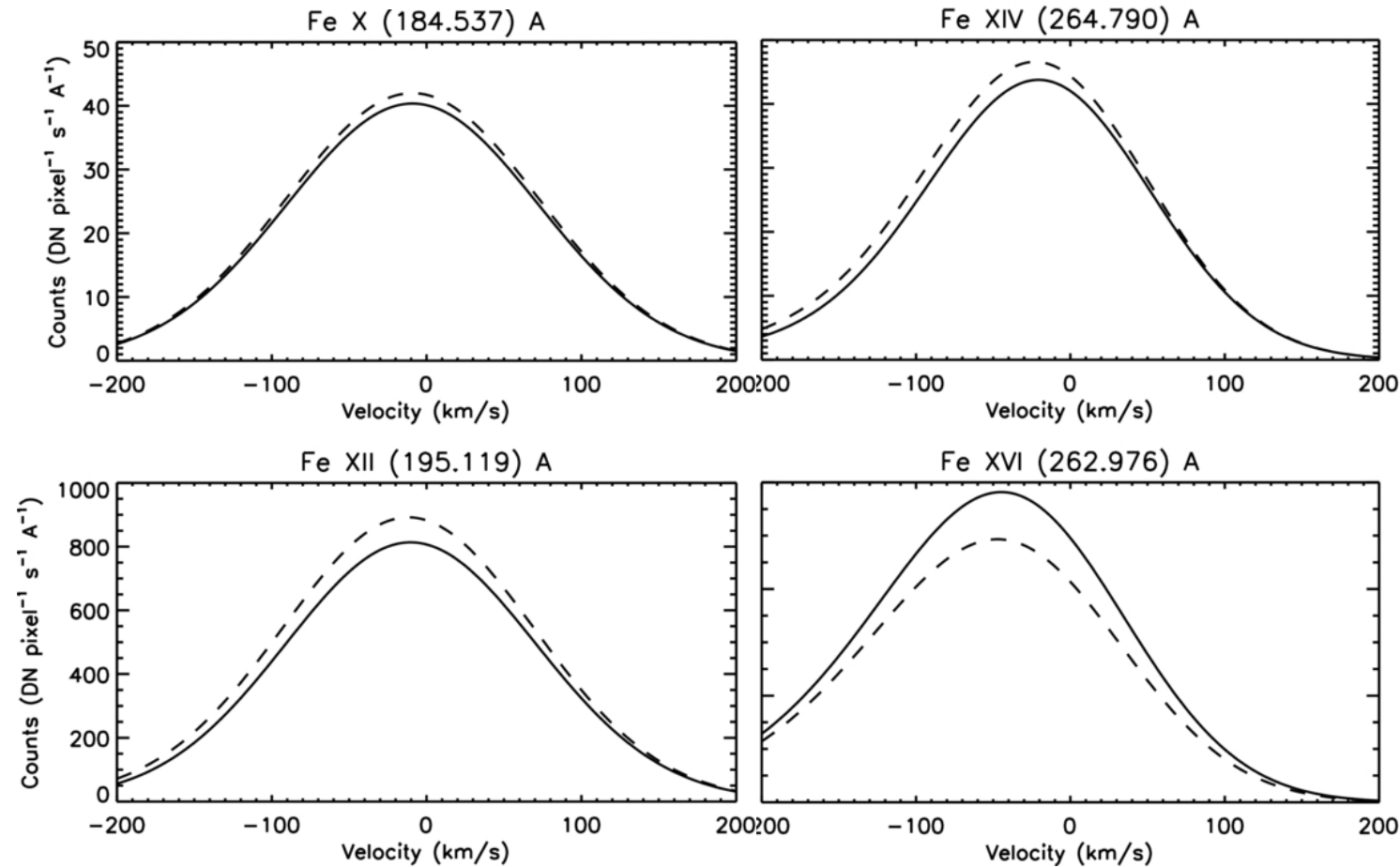


- Del Zanna et al. (2011) proposed that coronal outflows are due to interchange reconnection between high- pressure, closed loops in AR cores and adjacent low-pressure, open flux tubes.
- They found good agreement between the predicted and observed locations of the coronal outflows and the radio noise storms.

See also Baker et al. 2009

A fraction of the outflowing plasma contributes mass and momentum into the solar wind?

AR outflows as possible source of slow solar wind

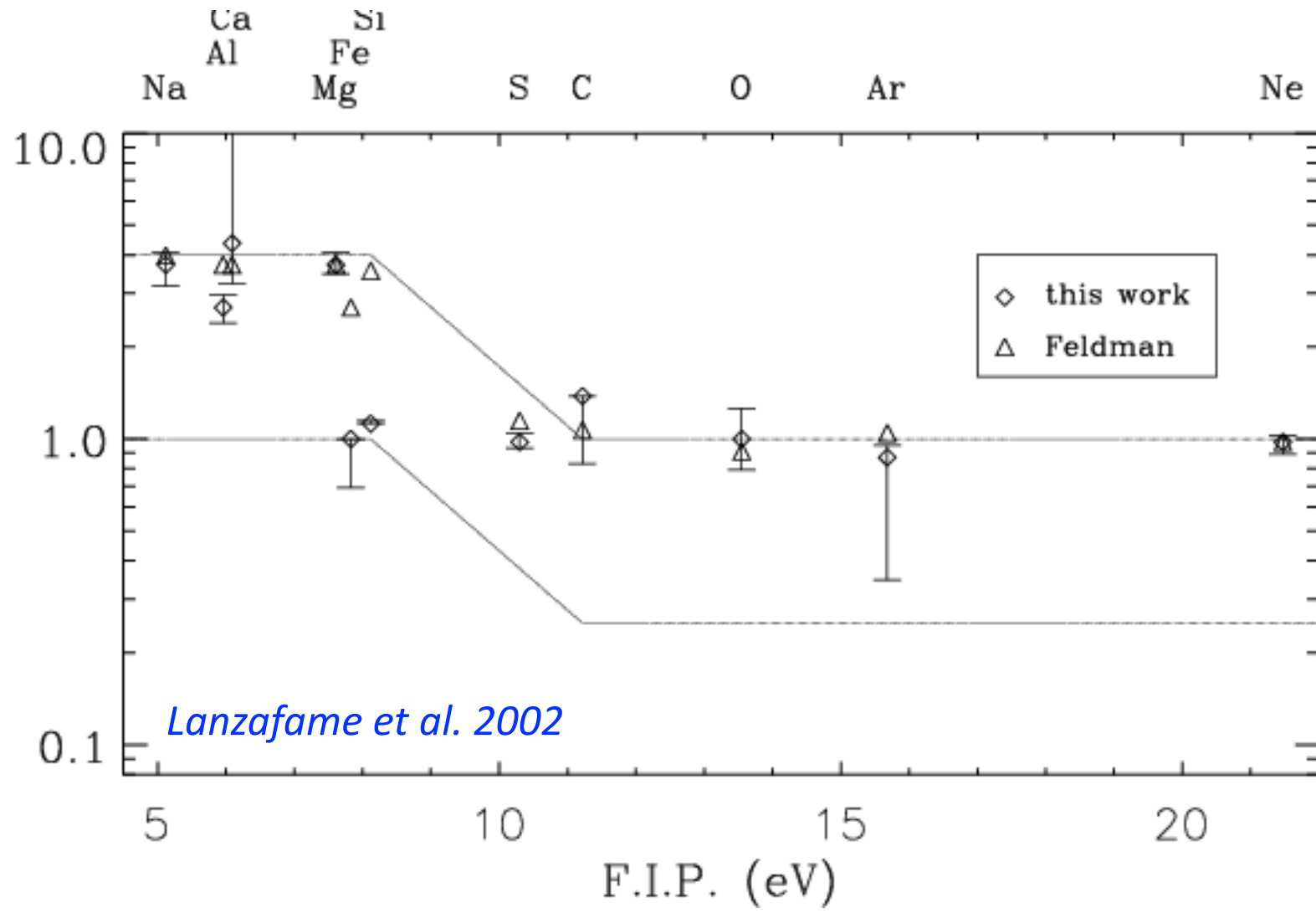


Bradshaw et al. 2011

- *Bradshaw et al. 2011* investigated the plausibility of the mechanism suggested by Del Zanna et al. 2011 by using 1D numerical radiative-hydrodynamic HYDRAD code (Bradshaw & Mason 1993) and forward-modeled of spectral lines for direct comparison with the EIS data
- They confirmed the the observed velocity versus temperature structure of the outflow regions, and found an *excellent agreement between the predicted and observed Fe XII 195.119 Å line profile*

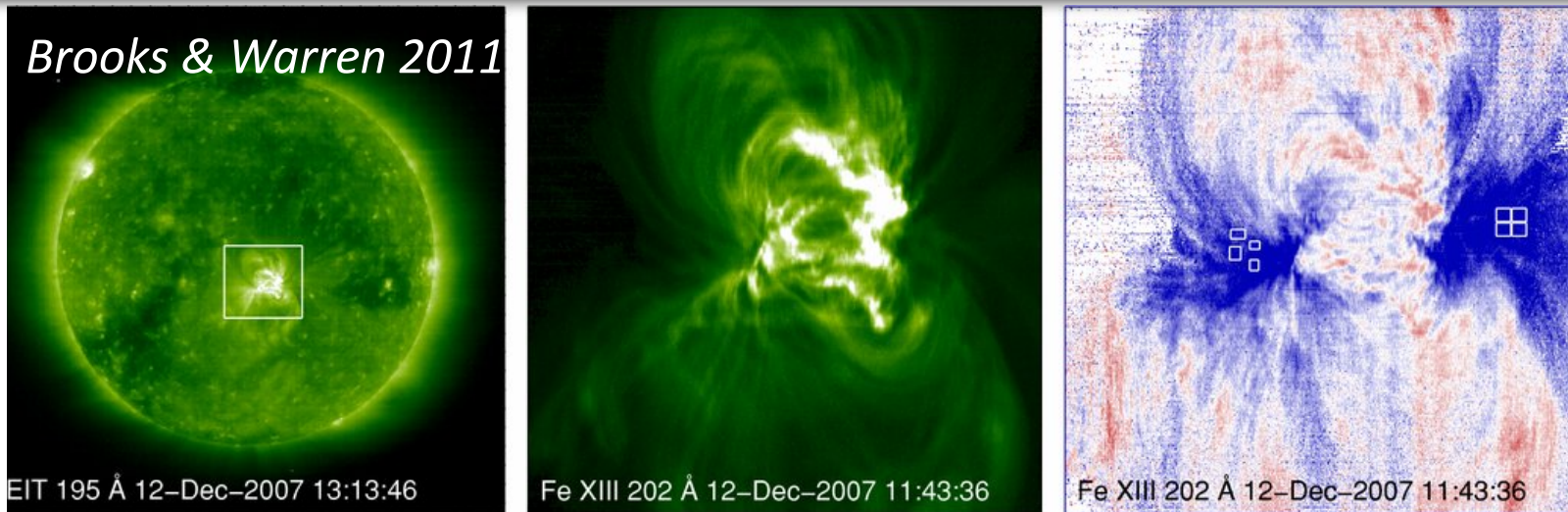
Abundances & FIP effect

Abundance/photospheric abundance



- In the slow solar wind elements with a first ionization potential (FIP) below about 10 eV are enhanced by factors of 3–4 relative to their photospheric abundances (von Steiger et al. 2000; Feldman & Widing 2003, Laming 2015).
- Abundances of fast solar wind are normally close to the photospheric ones, consistent with observations in coronal holes (von Steiger et al. 2000, Feldman & Laming 2000).

Abundances & FIP effect



EIS measurements confirms the composition of the outflows is consistent with slow wind values (Brooks & Warren 2011).

Properties of AR 10978 Outflows Measured in EIS Slit Scans

Date	Start Time	Location	v (km s ⁻¹)	η (km s ⁻¹)	$\log(N_e/\text{cm}^{-3})$	$\log(T_p/\text{K})$	f_{FIP}
2007 Dec 12	11:43:36	East	-16.6	39.7	8.7	6.2	4.0
			-12.6	32.9	8.6	6.2	3.5
			-17.3	39.0	8.6	5.6	3.8
			-20.4	41.0	8.7	6.3	4.1
		West	-18.1	40.4	8.5	6.2	3.1
			-20.8	43.3	8.5	6.2	3.7
			-21.8	45.8	8.5	6.2	3.4
			-22.3	47.3	8.5	6.2	3.8

- Si is always enhanced over S by a factor of 3-4.
- The Si/S ratio was found to match the value measured a few days later by the Advanced Composition Explorer (ACE)
- Photospheric abundances in polar coronal hole

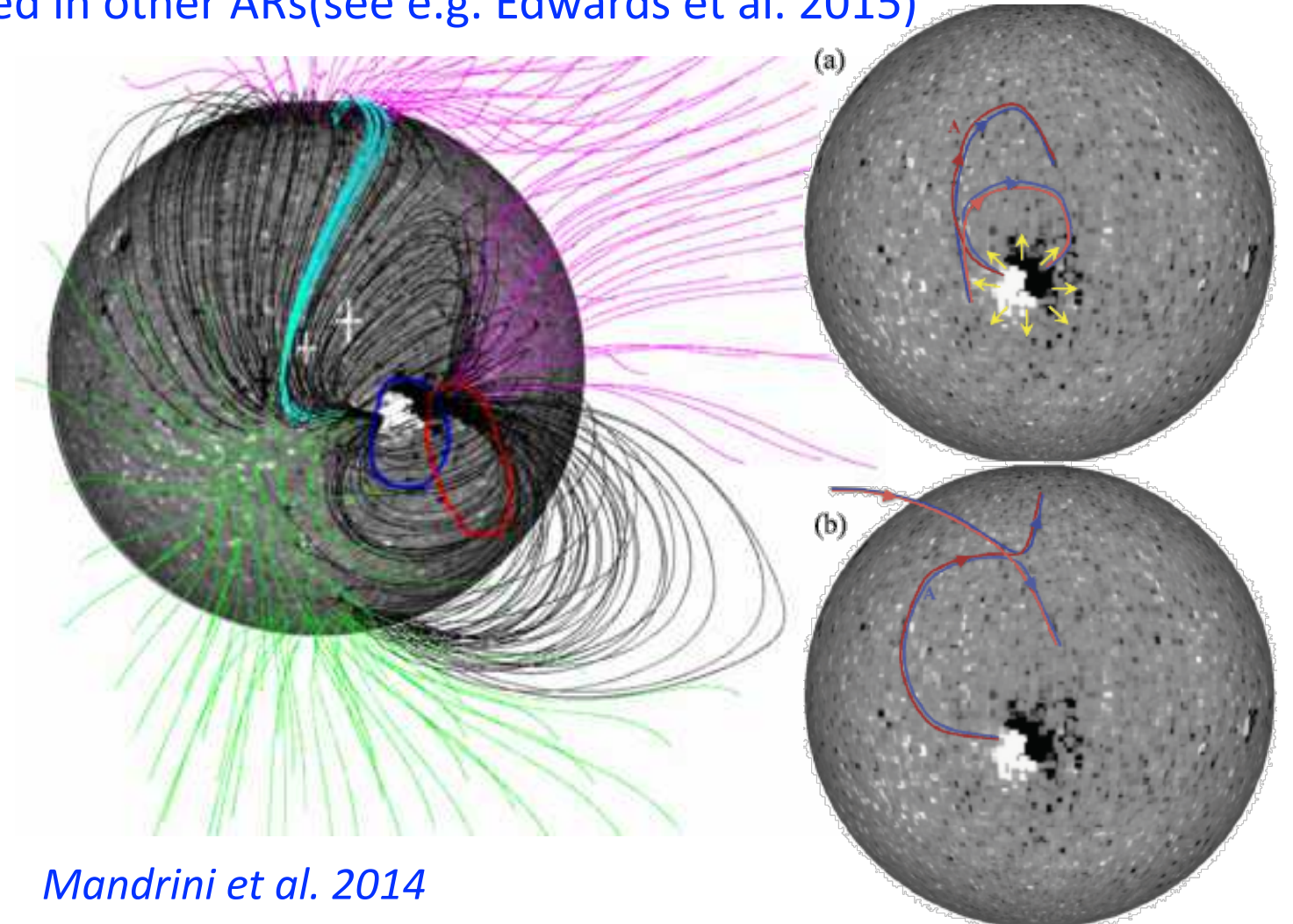
How does the plasma escape?

PFSS models showed that AR 10978 (Brooks & Warren 2011) was completely covered by the closed field of a helmet streamer with no topological link between plasma upflows and open field (Culhane et al. 2014). This has also been observed in other ARs (see e.g. Edwards et al. 2015)

2 step-reconnection process:

The upflowing plasma is first released in large-scale loops that later reconnect with open field, and finally, some of the AR plasma is detected *in-situ* by ACE (Culhane et al. 2014, Mandrini et al. 2014)

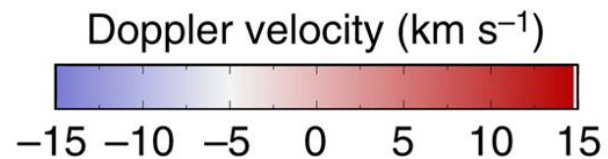
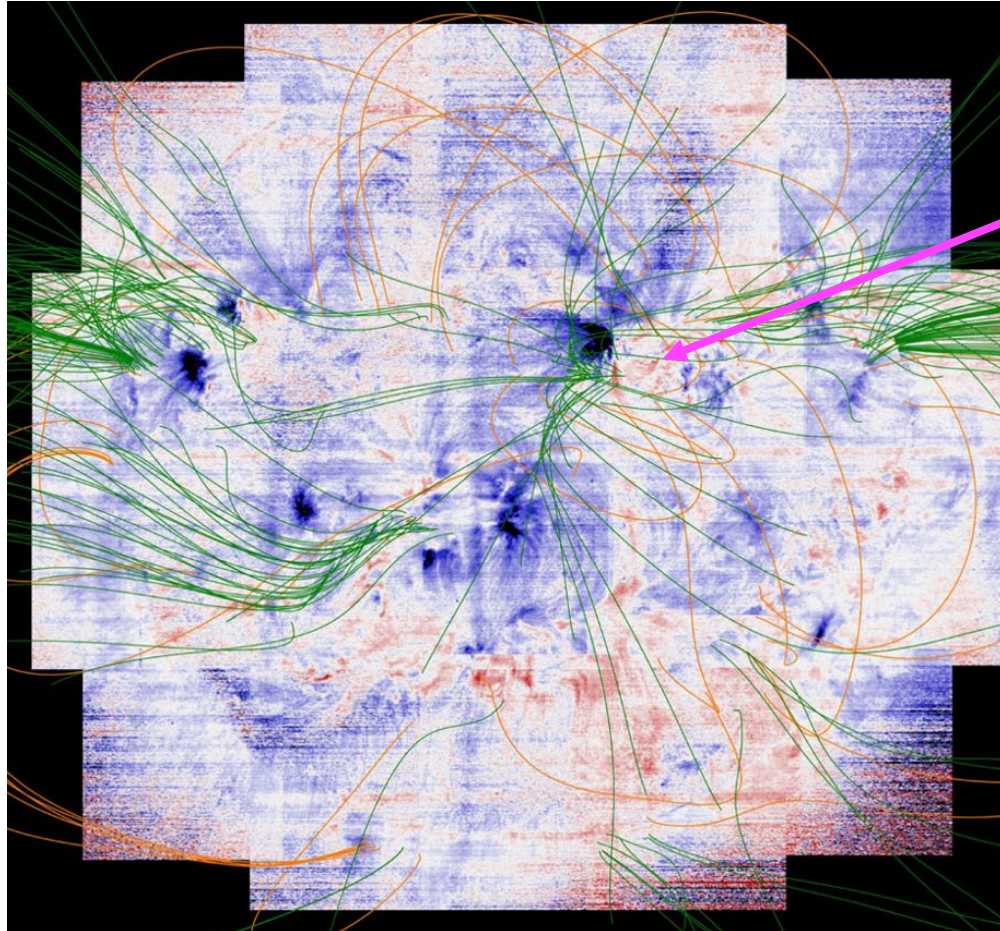
See also van Driel-Gesztelyi *et al.* ([2012](#))



Mandrini et al. 2014

Solar wind source map of the full Sun

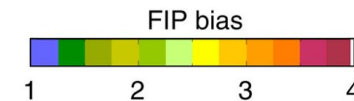
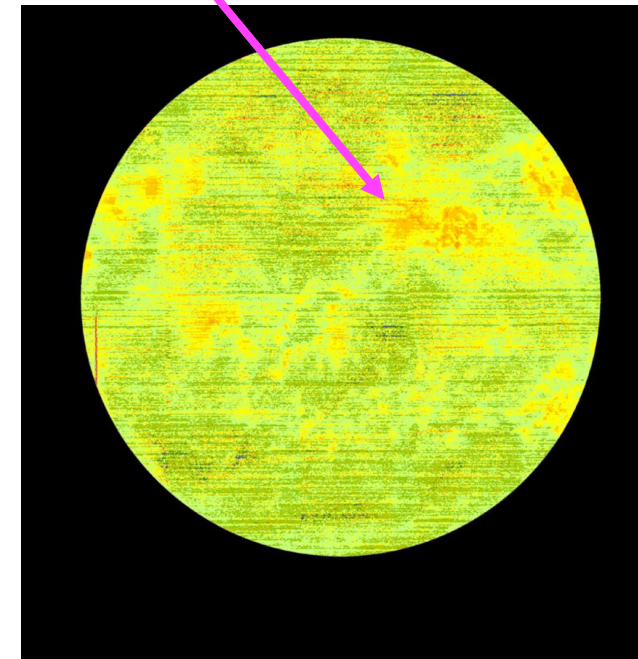
EIS Fe XII Doppler velocity map + PSFF extrapolation (De Rosa & Schrijver 2003)



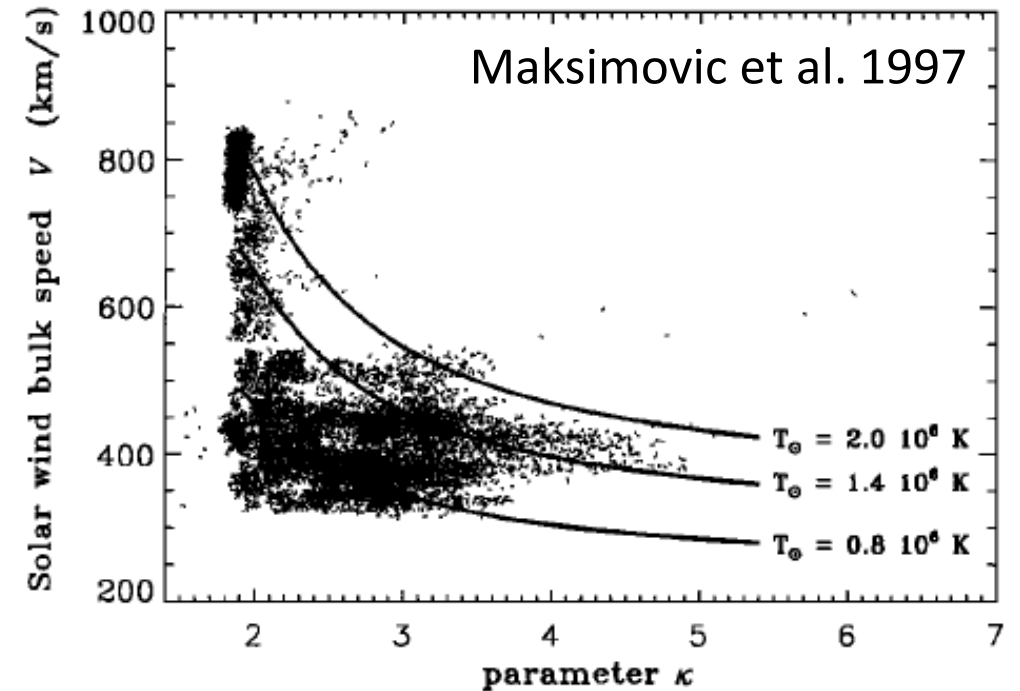
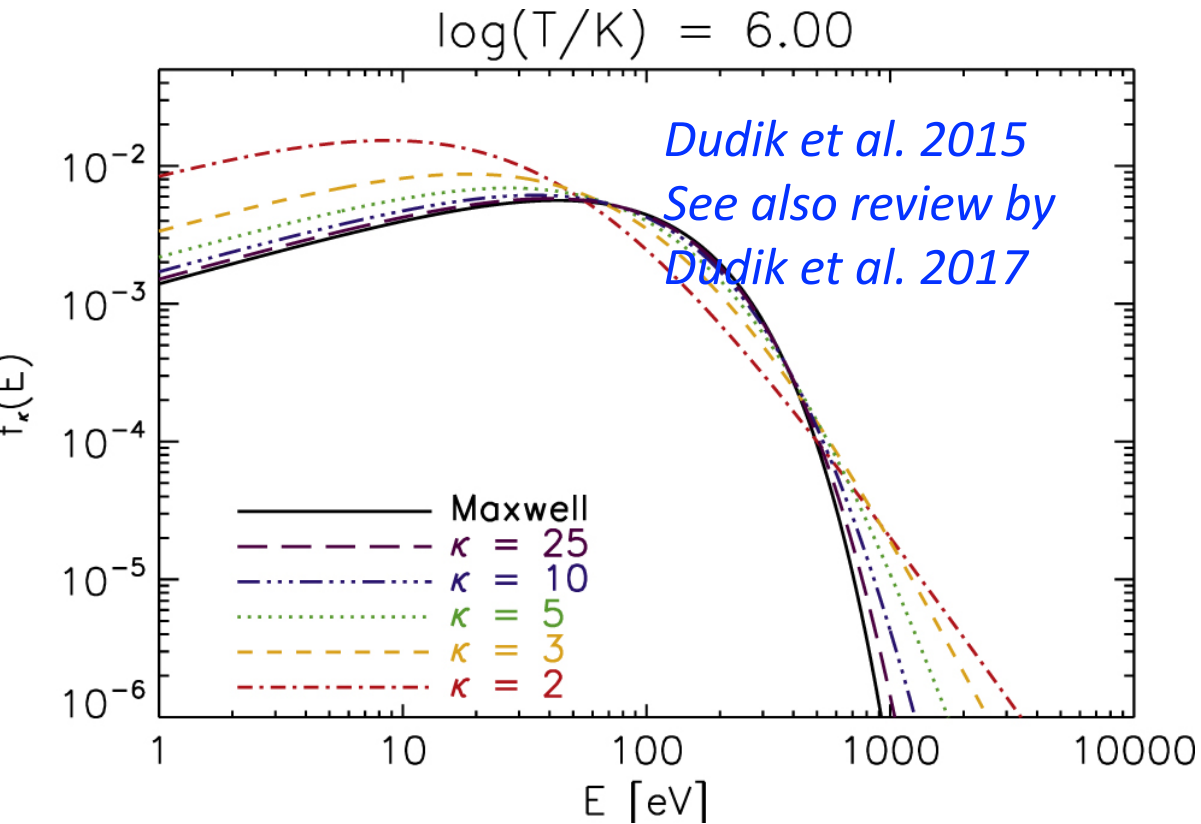
Brooks et al. 2015

Identify possible sources of slow solar wind by combining plasma composition for our full-Sun map

plasma composition of full-Sun map from the Si X 258.37/S X 264.22 Å ratio



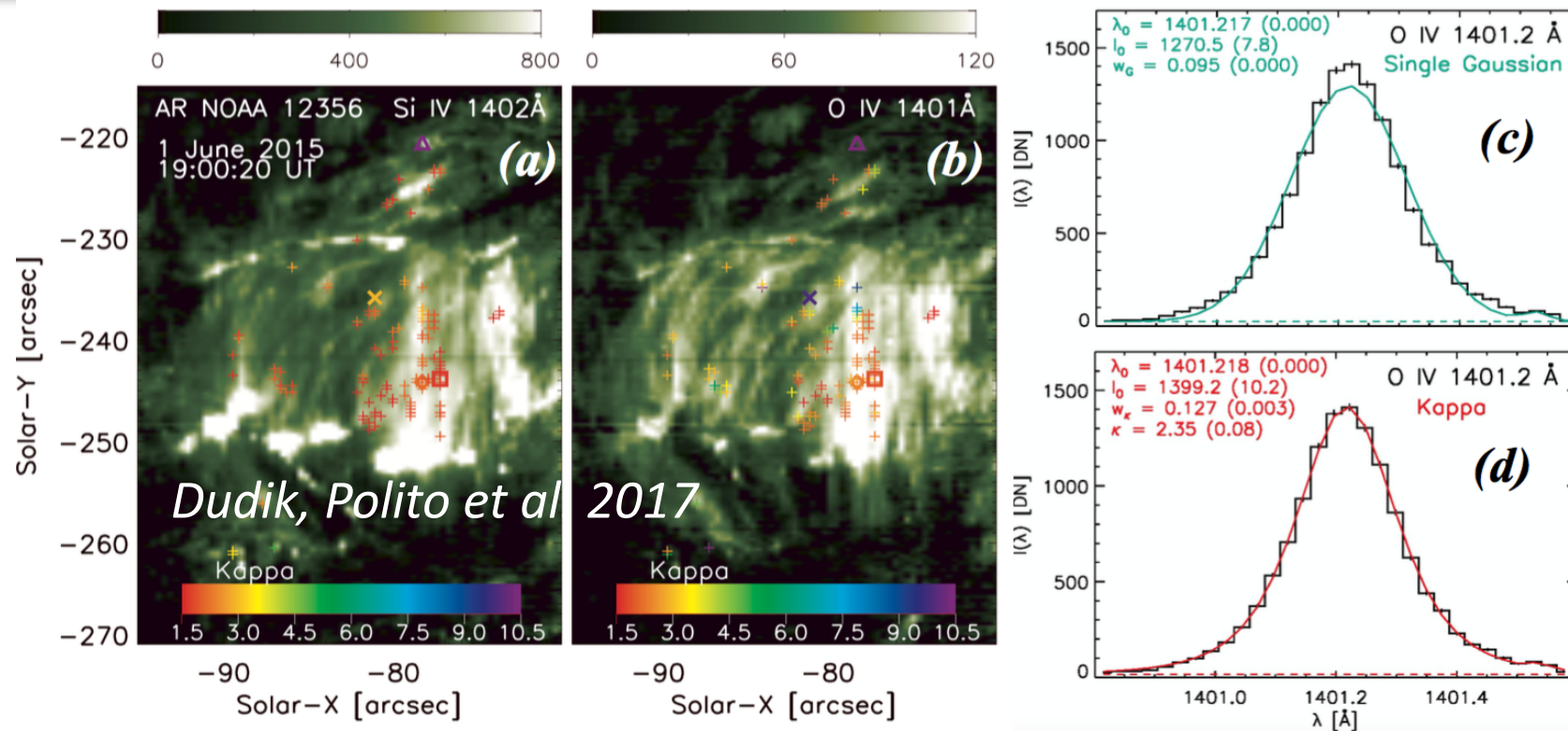
Non-Maxwellian (κ) diagnostics



Electron velocity distribution in the SW. There are two distinct populations: high speed solar wind streams with lower values of κ and low speed streams with larger values of κ

Evidence of non-Maxwellian κ -distributions has been found: in the *solar wind* (e.g. Collier et al. 1996; Maksimovic et al. 1997; Zouganelis 2008), *ARs* (Dzifčáková & Kulinová 2011, Testa et al. 2014, Dudik et al. 2017), *flares* (e.g. Oka et al. 2013, Jeffrey et al. 2017, Polito et al. 2018b)

Non-Maxwellian diagnostics in cool AR loops observed with IRIS



Signatures of non-Maxwellian distributions can be obtained from:

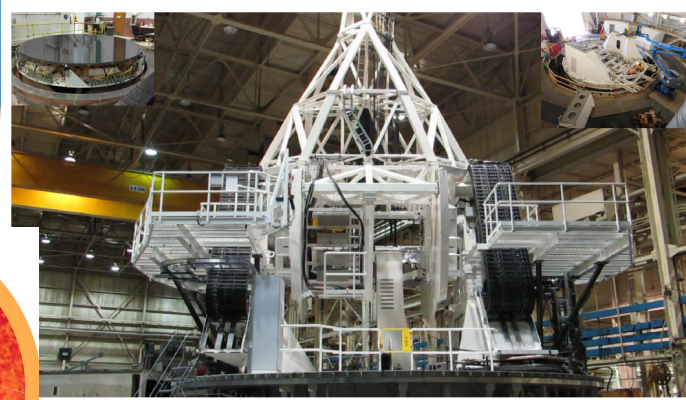
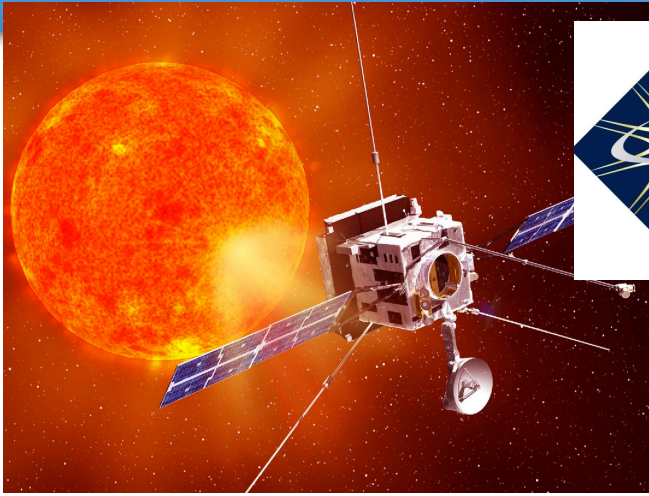
- *Line profiles* (ion distributions)
- *Intensity ratios* (electron distributions)

Detected non-Gaussian, highly symmetric profiles of TR lines in 120 pixels

- Typical κ values found from profiles are $\kappa \approx 1.7 - 2.5$
- Typical κ values found from fitting of relative intensities are $\kappa \approx 2 - 3$ (but sensitive to abundances)
- Jeffrey et al. 2018 found evidence of non-Maxwellian line profiles at the base of the fast solar wind in a coronal hole using EIS observations

See also Bahauddin's poster

Future instruments



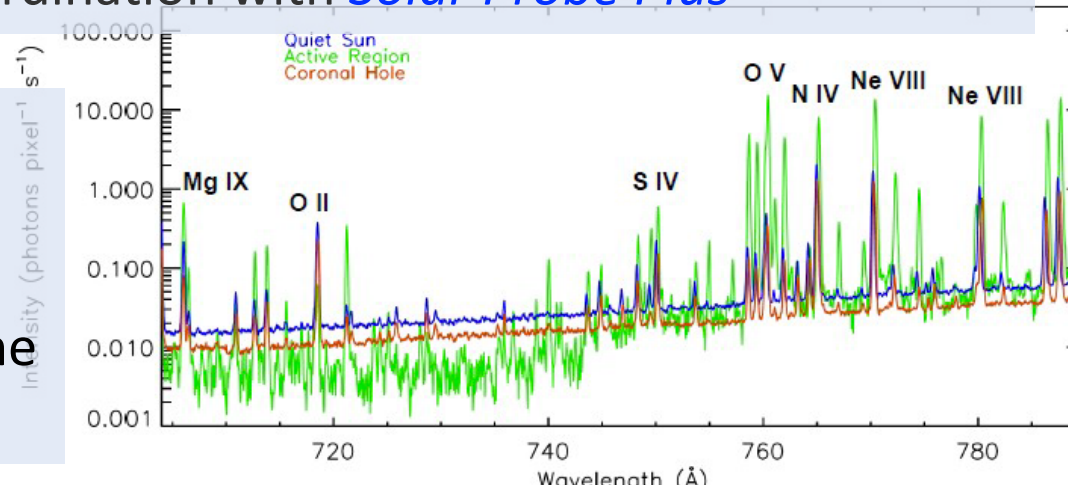
DKIST: potential for measuring Ne, Te, abundances, test for the presence of non-Maxwellian electrons in ARs (Dudik, Del Zanna et al., 2015, Del Zanna & De Luca 2017)

Solar Orbiter goal: understanding how the solar activity creates and influences the heliosphere by combining:

- in-situ instruments
- remote sensing instruments

Solar Orbiter will operate in coordination with *Solar Probe Plus*

The **SO/SPICE UV spectrometer** will remotely characterize the plasma properties at the solar surface - providing a link with the in-situ observations.



Wavelength (μm)	Line
→ 0.53	FeXIV
0.637	FeX
0.789	FeXI
→ 1.075	FeXIII
→ 1.083	HeI
1.25	S IX
→ 1.43	Si X
2.218	FeIX
2.326	CO
2.58	SiX
3.028	MgV III
→ 3.93	Si IX
→ 4.651	CO

Outlook

The origin of slow solar wind is still debated, crucial diagnostics will be provided by combining in-situ and remote sensing instruments:

- *Flows* (spectroscopy i.e. Hinode/EIS, SO/SPICE, IRIS, MUSE?)
- *FIP and chemical composition* (spectroscopy i.e. Hinode/EIS, SO/SPICE, IRIS, DKIST + in-situ with SO/SWA, PSP/SWEAP)
- *Context information on the ARs* (from imaging e.g., SDO-AIA, Hinode-XRT, SO/EUI)
- Signatures of *non-equilibrium conditions and non-thermal electrons* in the AR and SW (spectroscopy i.e. Hinode/EIS, SO/SPICE, IRIS, SO/STIX + in-situ from SO/EPD and SWA, PSP/ISOIS)
- *Magnetic field modeling* (SDO-HMI, SO/PHI, SO/MAG)

Discussion

- *How does the outflow plasma escape from ARs? What role does reconnection play in transporting plasma from closed coronal loops into the solar wind?*
- *Do signatures of the heating (e.g. chemical composition, non-Maxwellian electrons) in ARs persist in the slow solar wind? Are they observable? How can we connect them?*
- *How can future instruments be used to identify such signatures?*
- *What kinds of models are needed to understand the relationship between closed-field ARs and the slow wind?*